

Supplemental material

Fit projections for the normalisation channels

The $p\bar{p}hh'$, $p\bar{p}$ and hh' invariant-mass distributions of the $p\bar{p}K^+\pi^-$ and $p\bar{p}K^+K^-$ samples, from which the $J/\psi K^{*0}$ and $J/\psi\phi$ normalisation yields are extracted, are shown in Fig. 1 with the 3D fit projections superimposed.

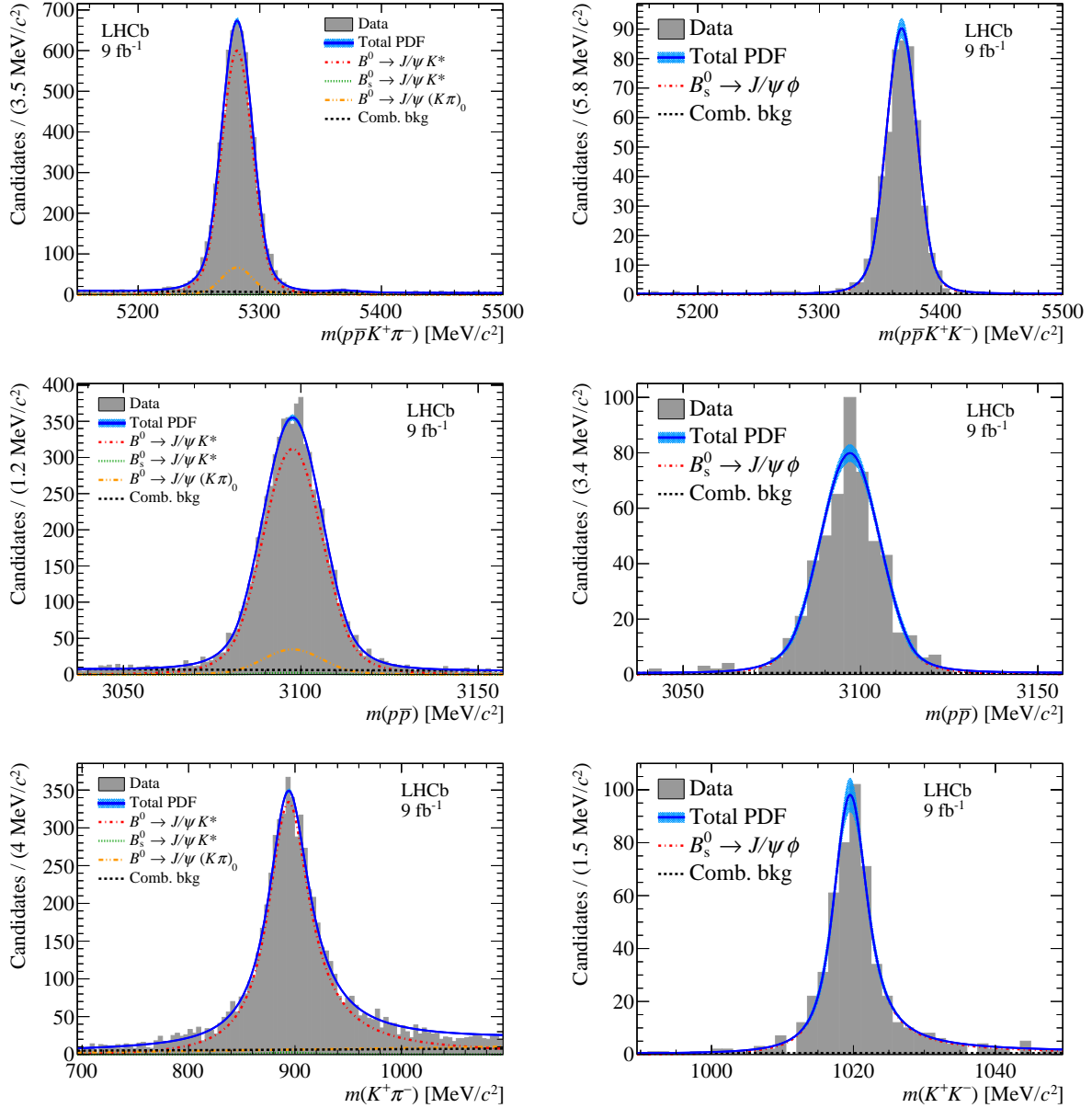


Figure 1: Distributions and 3D fit results of (top left) $m(p\bar{p}K^+\pi^-)$, (middle left) $m(p\bar{p})$ and (bottom left) $m(K^+\pi^-)$ from the $p\bar{p}K^+\pi^-$ data sample after the final tight selection, as well as the distributions and 3D fit results of (top right) $m(p\bar{p}K^+K^-)$, (middle right) $m(p\bar{p})$ and (bottom right) $m(K^+K^-)$ from the $p\bar{p}K^+K^-$ data sample after the final very tight selection. The hashed cyan band corresponds to the 1σ model uncertainty based on the fit covariance matrix.

Distributions of $m(p\bar{p})$ in the $p\bar{p}p\bar{p}$ sample

The $p\bar{p}$ invariant-mass distributions for the four $p\bar{p}$ pairs of the $p\bar{p}p\bar{p}$ sample are shown in Fig. 2 for signal enriched data with the requirements $|m_{p\bar{p}p\bar{p}} - 5282| < 30 \text{ MeV}/c^2$ together with the tight selection (B^0 mass region) and $|m_{p\bar{p}p\bar{p}} - 5365| < 30 \text{ MeV}/c^2$ with the very tight selection (B_s^0 mass region).

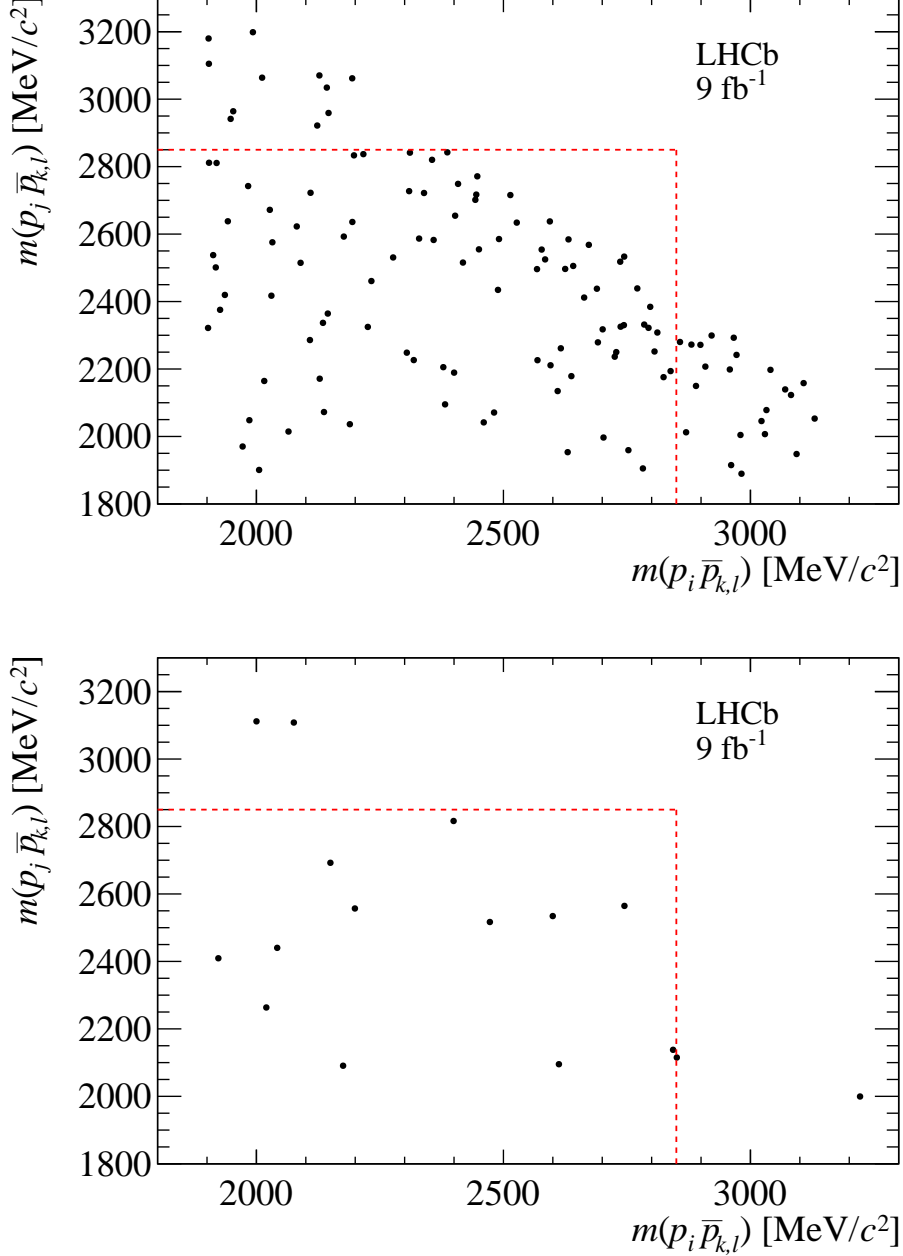


Figure 2: Two-dimensional invariant-mass distributions of all four combinations of $p\bar{p}$ pairs in the $p\bar{p}p\bar{p}$ data (two entries per candidate) with (top) the tight selection and $|m_{p\bar{p}p\bar{p}} - 5282| < 30 \text{ MeV}/c^2$, and (bottom) the very tight selection and $|m_{p\bar{p}p\bar{p}} - 5365| < 30 \text{ MeV}/c^2$. Data outside the red-dashed lines are excluded by the $c\bar{c}$ veto.